Check for updates

Korean Journal of Radiology

KJR

Cone-Beam Computed Tomography-Hepatic Arteriography as a Diagnostic Tool for Small Hypervascular Hepatocellular Carcinomas: Method and Clinical Implications

Ye Ra Choi, MD[1], Jin Wook Chung, MD, PhD[2], Jung Hoon Kim, MD[2], Hyo-Cheol Kim, MD, PhD[2], Hwan Jun Jae, MD, PhD[2], Saebeom Hur, MD[2]

[1]Department of Radiology, Seoul National University-Seoul Metropolitan Government Boramae Medical Center, Seoul, Korea; [2]Department of Radiology, Seoul National University Hospital, Seoul, Korea

Objective: This study proposes a novel reference standard for hypervascular hepatocellular carcinomas (HCCs), established by cone-beam computed tomography-hepatic arteriography (CBCT-HA) and two-year imaging follow-up, and discusses its clinical implication on tumor staging and understanding the intrahepatic distant recurrence (IDR) in relation to dynamic computed tomography (CT).

Materials and Methods: In this retrospective study, 99 patients were enrolled, who underwent CBCT-HA during initial chemoembolization for HCC suspected on CT. All patients underwent chemoembolization and regular clinical and imaging follow-up for two years. If IDR appeared on follow-up imaging, initial CBCT-HA images were reviewed to determine if a hypervascular focus pre-existed at the site of recurrence. Pre-existing hypervascular foci on CBCT-HA were regarded as HCCs in initial presentation. Initial HCCs were classified into three groups according to their mode of detection (Group I, detected on CT and CBCT-HA; Group II, additionally detected on CBCT-HA; Group III, confirmed by interval growth). We assessed the influence of CBCT-HA and two-year follow-up on initial tumor stage and calculated the proportion of IDR that pre-existed in initial CBCT-HA.

Results: A total of 405 nodules were confirmed as HCCs, and 297 nodules initially pre-existed. Of the initial 297 HCCs, 149 (50.2%) lesions were in Group I, 74 (24.9%) lesions were in Group II, and the remaining 74 (24.9%) lesions were in Group III. After applying CBCT-HA findings, 11 patients upstaged in T stage, and 4 patients had a change in Milan criteria. Our reference standard for HCC indicated that 120 of 148 (81.1%) one-year IDR and 148 of 256 (57.8%) two-year IDR existed on initial CBCT-HA.

Conclusion: The proposed method enabled the confirmation of many sub-centimeter-sized, faintly vascularized HCC nodules that pre-existed initially but clinically manifested as IDR. Our reference standard for HCC helped in understanding the nature of IDR and the early development of HCC as well as the clinical impact of tumor staging and treatment decision.

Keywords: *Cone-beam CT-hepatic arteriography; Dynamic CT; Hypervascular hepatocellular carcinoma; Initial tumor stage; Intrahepatic distant recurrence*

INTRODUCTION

Hepatocellular carcinoma (HCC) is the sixth most common cancer worldwide, and the third most common cause of death due to cancer (1). Recent advances in imaging technology enable HCC to be diagnosed without biopsy if a tumor nodule is greater than 1 cm in diameter and shows typical arterial enhancement with delayed washout on dynamic computed tomography (CT) or magnetic resonance imaging (MRI). However, it is still difficult to make a correct diagnosis using imaging techniques or biopsy for sub-centimeter-sized HCCs, because diagnostic accuracy decreases with the diminishing size of nodules due to false-positive results, such as small hemangiomas, regenerative nodules, arterioportal shunts, and inadequate specimens (2-8). Diagnosis using thin-section, whole-explant correlation following transplantation has been established as a standard reference to diagnose HCC; however, it remains a treatment option for only a limited number of patients (9, 10). In addition, a complete correlation between pathology and imaging findings is difficult to perform in clinical practice. Consequently, the characteristics or behavior of sub-centimeter-sized HCCs are not well understood.

Early diagnosis of HCC remains important for improving the disease prognosis. The development of cone-beam computed tomography (CBCT) using a flat-panel detector has increased the detection of hypervascular HCC nodules, when used in conjunction with standard digital subtraction angiography (DSA), during transcatheter arterial chemoembolization (TACE) (11-13). CBCT-hepatic arteriography (CBCT-HA) can better visualize tumor-feeding vessels, as well as provide better information regarding tumor vascularity, as compared with CT, because it provides high lesion-to-background contrast and spatial resolution (14-18).

This study proposes a novel reference standard for hypervascular HCC, established by CBCT-HA and two-year imaging follow-up, and discusses its clinical implication on tumor staging and understanding the intrahepatic distant recurrence (IDR) in relation to dynamic CT.

MATERIALS AND METHODS

Patient Selection

The present study was retrospective in nature, which was approved by our Institutional Review Board, and the informed consent was waived. The study included 276 patients suspected of having HCC, on the basis of the clinical presentation and radiologic findings, and who were referred to undergo their first TACE treatment, between June 2009 and June 2010. A total of 89 patients were excluded (54 patients who underwent CT at an outside hospital, 25 patients who underwent CT with more than a two-month interval between TACE, and 10 patients with inadequate dynamic CT protocol). We then selected 187 patients who underwent dynamic liver CT at our hospital, less than two months before TACE. We also excluded 22 patients with diffuse HCC (n = 9), more than 10 HCC lesions (n = 5), portal vein thrombosis (n = 3), or extrahepatic metastasis (n = 5), as seen on initial CT. With regard to performing CBCT-HA before chemoembolization, we excluded 51 patients that required multiple injections for whole-liver scanning, due to a separate hepatic arterial supply. In addition, we also excluded 11 patients with blurring on CBCT-HA images, due to motion artifact. Of the remaining 103 patients, we excluded four patients who did not undergo chemoembolization in the initial session, due to the absence of hypervascular HCC seen on CBCT-HA. Therefore, the final study group consisted of 99 patients (81 men and 18 women; mean age 63.6 ± 8.3). The mean time interval between initial CT and the CBCT was 19 days (0–59 days).

Clinical Follow-Up

In all 99 patients, dynamic liver CT was performed every three months, in addition to the clinical surveillance used to detect tumor recurrence after the initial TACE. During the two-year follow-up period, if a hypervascular HCC was newly suspected, TACE was performed with CBCT assistance in routine clinical practice. Laboratory data included aspartate transaminase, alanine transaminase, albumin, total bilirubin, prothrombin time/international normalized ratio, and platelet count. The serum tumor marker alpha-fetoprotein (AFP) level was also evaluated every three months, in addition to radiologic examinations.

CBCT Techniques

TACE procedures were performed using a CBCT-capable angiography unit (AXIOM Artis dTA/VB30, Siemens Healthineers, Erlangen, Germany), with a 30 x 40 cm, flat-panel detector. Before C-arm scanning, selective arterial DSA of the celiac trunk or common hepatic artery was performed (5-Fr RH catheter, Cook, Bloomington, IN, USA), to examine the vascular anatomy and blood flow. Following DSA, C-arm CT images of the hepatic artery were

obtained during a single breath-hold, and with 211° of circular trajectory, for eight seconds (5-Fr RH catheter; 4-Fr Glidecath, Terumo, Tokyo, Japan; 2.7-Fr Radio Star, Taewoong Medical Co., Gimpo, Korea; 2.4-Fr MicroFerret, Cook). Contrast-enhanced images were acquired using undiluted, iodinated contrast medium (iopamidol; Pamiray 300, Dongkook Pharmaceutical, Seoul, Korea), at a flow rate of 1.5–6 mL/s for 12 seconds, with a 4- or 6-second x-ray delay. The CBCT-HA acquisition protocol was: 0.5° increment; 512 x 512 matrix in projections; 210° total angle at approximately 26° per second; a system dose of approximately 0.36 μGy per frame; and a total of 419 projections. The raw datasets from the angiography system were transferred to a dedicated external workstation (Leonardo with DynaCT, Siemens Healthineers), where the two-dimensional axial, coronal, and sagittal multiplanar reformation images were reconstructed with 1-mm slice thickness and three-dimensional volume-rendering, or where the maximum intensity projection images were reformed.

Novel Reference Standard to Identify Hypervascular HCCs at the Initial and during the Follow-Up Period

In order to confirm hypervascular HCCs, two radiologists (with 20 years of clinical experience in interventional radiology, and with 4 years of clinical experience in radiology) retrospectively reviewed all CT and CBCT-HA images at the initial presentation, as well as consecutive CT, MRI, and CBCT-HA images obtained during a two-year follow-up period, by consensus opinion. In addition, the same radiologists retrospectively reviewed the formal reports of all 99 patients, in order to evaluate whether the diagnosis of HCC was made in the initial dynamic CT.

The two ways to identify HCC at the initial presentation were as follows. First, we evaluated whether the compact iodized oil uptake was observed on consecutive follow-up CT scans for hypervascular nodules presented on the initial CT or CBCT-HA, and treated with TACE at the initial session. A nodule was considered HCC if nodular iodized oil uptake was continued for at least one year of follow-up. Second, we reviewed the initial CBCT-HA images and determined whether a hypervascular focus was pre-existing at the recurrence site for IDR developed during a two-year follow-up period. Matched pre-existing hypervascular foci on CBCT-HA were considered HCCs at the initial presentation with interval growth. IDR was defined as the development of new lesions that were not detected in initial dynamic CT, and was determined from confirmative findings in subsequent dynamic CT or MRI, and treatment with TACE.

HCC Categorization Based on Mode of Detection

On the retrospective review of formal reports of the initial dynamic liver CT, the two radiologists categorized initial i.e., HCCs into three groups, based on the mode of detection for HCC (i.e., how and when HCCs were detected during clinical and imaging follow-up). Group I consisted of nodules reported as definite or probable HCCs on initial dynamic CT. Group II consisted of HCCs additionally detected on CBCT-HA, and treated with CBCT-assisted TACE. Group III consisted of HCCs that pre-existed as hypervascular foci on initial CBCT-HA, and showed interval growth on follow-up CT or MRI. Group III HCCs were suspected after interval growth during the follow-up period, and were subsequently treated with TACE (Fig.1).

Impact of CBCT-HA and Two-Year Clinical Follow-Up on Initial Tumor Stage and IDR

We assessed the influence of CBCT-HA and two-year clinical follow-up on initial tumor stage (American Joint Committee on Cancer/Union for International Cancer Control [AJCC/UICC] tumor, node and metastasis [TNM] staging system and Milan criteria) (19, 20). We also analyzed IDR that occurred during the two-year follow-up period. For all IDR nodules, we sought to identify HCCs presented in the initial CBCT-HA, and to calculate the proportion of IDR that pre-existed in the initial CBCT-HA.

Statistical Analysis

The basic clinical characteristics and radiologic evaluation of patients were described as the mean value, with standard deviations and frequencies. All statistical analyses were performed using Statistical Package for Social Science (SPSS version 19.0, IBM Corp., Armonk, NY, USA).

RESULTS

The baseline characteristics of the 99 patients are summarized in Table 1. During two-year follow-up, a total of 405 nodules, except for disseminated recurrence in five patients, were confirmed as hypervascular HCCs. Of the total 405 HCCs, 297 HCCs in 99 patients were identified as present in the initial examination, and 108 HCCs occurred *de novo* during the follow-up period. Of the initial 297 HCC lesions in 99 patients, 40 patients had a single lesion, 24 had 2 lesions, 11 had 3 lesions, 7 had 4 lesions, 14 had
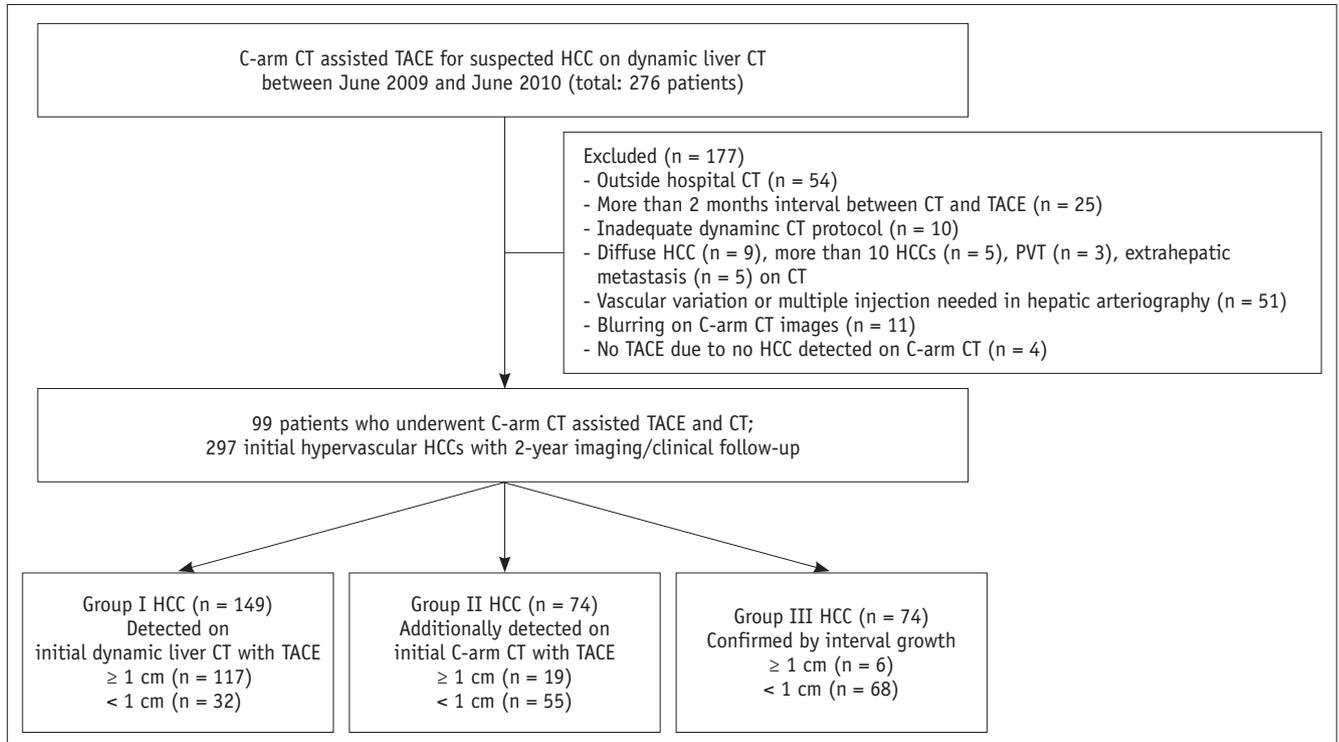
Fig. 1. Flowchart shows study group inclusion process. HCC = hepatocellular carcinoma, PVT = portal vein thrombosis, TACE = transcatheter arterial chemoembolization

5 to 10 lesions, and 3 had more than 10 lesions on CBCT-HA. Of the total 297 initial HCCs, 142 (47.8%) lesions were larger than or equal to 1 cm and 155 (52.2%) lesions were smaller than 1 cm. The mean diameter of all HCCs was 13.3 ± 12.3 mm.

HCC Categorization Based on Mode of Detection

Of the 297 HCCs, 149 (50.2%) lesions in 92 patients were Group I lesions, detected on initial dynamic CT, and treated with TACE; 74 (24.9%) lesions in 24 patients were Group II lesions, additionally detected on CBCT-HA, and treated with TACE; and the remaining 74 (24.9%) lesions in 39 patients were Group III lesions that pre-existed as hypervascular foci on initial CBCT-HA, and showed interval growth on follow-up CT or MRI (Table 2, Fig. 2). The mean diameter of each group of HCCs was 19.1 ± 14.9 mm (Group I), 8.2 ± 3.3 mm (Group II), and 6.4 ± 2.9 mm (Group III). The average HCC size after the interval growth of Group III HCCs was 11.4 mm, and the mean growth interval was 10.1 ± 6.8 months. Figure 3 illustrates an example of a patient with both group I, II, and III nodules.

Based on the dynamic CT, the initial T stages of HCC for all patients were T1a in 45 patients, T1b in 20 patients, T2 in 31 patients, and T3 in 3 patients. According to Milan criteria, the initial stages were single HCC within Milan in 61 patients, single HCC beyond Milan in 4 patients, multiple HCCs within Milan in 24 patients, and multiple HCCs beyond Milan in 10 patients.

Impact of CBCT-Based Novel Standard on Initial Tumor Staging and IDR

The initial T stages based on CBCT-HA with Group II lesions were T1a in 35 patients, T1b in 19 patients, T2 in 41 patients, and T3 in 4 patients. According to Milan criteria, the initial stages were single HCC within Milan in 50 patients, single HCC beyond Milan in 4 patients, multiple HCCs within Milan in 34 patients, and multiple HCCs beyond Milan in 11 patients. T stages were changed from T1a to T2 in 10 patients, from T1b to T3 in 1 patient, and Milan criteria were changed from within to beyond in 4 patients, in comparison with initial CT staging.

Based on our reference standard including Group II and III lesions, the initial T stages were T1a in 23 patients, T1b in 17 patients, T2 in 54 patients, and T3 in 5 patients. By Milan criteria, the initial stages were single HCC within Milan in 38 patients, single HCC beyond Milan in 2 patients, multiple HCCs within Milan in 30 patients, and multiple HCCs beyond Milan in 29 patients. T stages were changed

Table 1. Baseline Characteristics of Patients

Parameters	All (n = 99)
Age	63.6 ± 8.3*
Sex (male/female)	81/18
Etiology	
HBV-related	71
HCV-related	20
Others	8
Albumin (g/dL)	3.53 ± 0.54
Total bilirubin (mg/dL)	1.12 ± 0.64
Prothrombin activity (INR)	1.24 ± 0.18
Thrombocytopenia† (absent/present)	40/59
Splenomegaly‡ (absent/present)	57/42
Portal hypertension by EPS sign§ (absent/present)	45/54
Ascites (absent/present)	86/13
Child-Pugh score	
A5	48
A6	27
B7	18
B8–C10	6
MELD score	
≤ 9	61
10–19	35
20–29	3
AFP (≤ 200 ng/mL / > 200 ng/mL)	78/21
Previous treatment	
PEIT	25
RFA	25
Operation	16
Number of tumors	3.00 ± 3.52
Tumor multiplicity (single/multiple)	CT (65/34), CBCT-HA (40/59)
Maximum tumor size (cm)	2.30 ± 1.65
0.1–1.0	9
1.1–2.0	50
2.1–5.0	33
5.1–10.0	7
BCLC staging	
0	19
A	56
B	24
T stage (AJCC/UICC)	CT/CBCT-HA
T1a	45/35
T1b	20/19
T2	31/41
T3	3/4
Milan criteria (within/beyond)	CT (85/14), CBCT-HA (84/15)

*Values are means ± standard deviation, †Platelet count < 100 K/mm³, ‡Spleen size > 12 cm, §EPS sign means presence of endoscopy signs of gastro-esophageal varices and/or presence of thrombocytopenia with splenomegaly. AFP = alpha-fetoprotein, AJCC = American Joint Committee on Cancer, BCLC = Barcelona Clinic Liver Cancer, CBCT-HA = cone-beam computed tomography-hepatic arteriography, HBV = hepatitis B virus, HCV = hepatitis C virus, INR = international normalized ratio, MELD = model for end-stage liver disease, PEIT = percutaneous ethanol injection, RFA = radiofrequency ablation, UICC = Union for International Cancer Control

from T1a to T2 in 20 patients, from T1b to T2 in 2, and T1b to T3 in 2. By Milan criteria, 17 patients changed from within to beyond the criteria.

According to our definition of IDR (new lesions not detected in initial dynamic CT), including Group II, III, and *de novo* HCCs, the number of IDR lesions was 148 in 50 patients and 256 in 68 patients during the one-year and two-year follow-up, respectively. Among the IDR lesions, 120 (81.1%) of one-year IDR (n = 148) and 148 (57.8%) of two-year IDR (n = 256) were present in the initial CBCT-HA (Table 3).

If IDR is alternatively defined as the development of new lesion after initial TACE, the 74 lesions in Group II should be excluded from IDR lesions. According to this definition, the number of IDR lesions was 74 in 42 patients and 182 in 64 patients during one-year and two-year follow-up, respectively. Among the IDR lesions by excluding Group II lesions, 46 (62.2%) of one-year IDR (n = 74) and 74 (40.7%) of two-year IDR (n = 182) were present in the initial CBCT-HA.

Table 3 summarizes the initial stages according to the dynamic CT and CBCT-based novel standard, and the proportion of pre-existing HCCs in initial CBCT-HA to IDR.

DISCUSSION

The current study demonstrated the role of CBCT-HA in depicting additional HCC lesions to CT, during the initial chemoembolization session. Using CBCT-HA, 74 (24.9%) HCC lesions (Group II) were additionally detected and treated at initial TACE, and another 74 (24.9%) lesions (Group III) were confirmed to be HCCs with interval growth during two-year clinical follow-up. Previous studies have reported that CBCT showed diagnostic accuracy, comparable or superior to dynamic CT (21, 22). Iwazawa et al. (22) showed that CBCT depicts hypervascular HCCs smaller than 10 mm in diameter more accurately than biphasic multidetector computed tomography (MDCT) (A_z = 0.830 vs. 0.618, $p < 0.001$). Higashihara et al. (21) also reported that the mean area under the alternative free-response receiver operating characteristic did not differ significantly between MDCT and CBCT (mean A_z, 0.83 vs. 0.85, $p = 0.32$). In their reports, the standard of reference for HCC was based on the findings of accumulation of iodized oil in a tumor seen on unenhanced CT. In our study, because of applying two-year follow-up results to the initial CBCT-HA findings, additional HCCs could be diagnosed. Therefore, our reference standard

Table 2. Mode of Detection and Number of HCCs during 2-Year Clinical Follow-Up

Number of HCCs	Initial Dynamic CT	First Detected on Initial CBCT-HA and Treated with TACE	Detected during 2-Year Clinical Follow-Up		Total
			At 1-Year	At 2-Year	
Number of HCCs preexisting on initial CBCT-HA	149*	74†	74‡(interval growth of preexisting lesion on initial CBCT-HA)		297
			46	28	
Number of de novo HCCs	-	-	108		108
			28	80	

*Group I HCC, †Group II HCC, ‡Group III HCC. HCC = hepatocellular carcinoma, TACE = transcatheter arterial chemoembolization
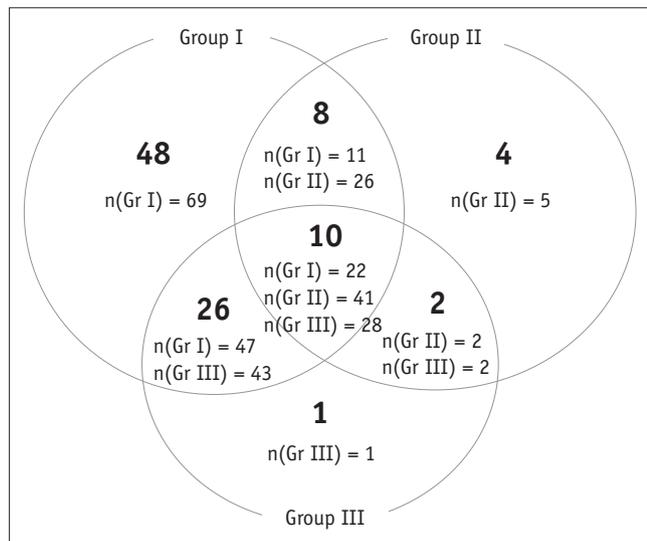
Fig. 2. Number of patients with nodules in each group. n(Gr #) = number of nodules in group #

for HCC using CBCT-HA and two-year clinical follow-up has been proven to have the potential to depict early-stage subclinical HCCs.

Our study results indicate that adding CBCT-HA may have a clinical impact on tumor staging, and further affect the therapeutic decision-making at the initial diagnostic workup. After applying CBCT-HA findings to CT, progression in the initial T stage was found in 11 patients, and change in the Milan criteria was found in 4 patients. These results suggest that changes in tumor staging due to additional nodules seen on CBCT-HA during chemoembolization, would affect patient prognosis and long-term survival. Regarding the initial staging analyses of HCC, recent studies have reported the usefulness of gadolinium ethoxybenzyl-diethylenetriaminepentaacetic acid (Gd-EOB-DTPA)-enhanced MRI, on staging and decision-making regarding treatment options for HCC (23-25). In the study by Jin et al. (23), new HCC lesions were additionally detected by Gd-EOB-DTPA-enhanced MRI in 17.3% of patients. In addition, the HCC stage has been reported to be revised in 11.5%

of patients after Gd-EOB-DTPA-enhanced MRI using the Barcelona Clinic Liver Cancer staging system (26). Yoo et al. (24) also reported that 33.3% of treatment decisions were changed after additionally using Gd-EOB-DTPA-enhanced MRI in patients with early-stage HCC. In their study, 12.1% of patients eligible for liver transplantation exceeded the Milan criteria, after detecting additional HCC by Gd-EOB-DTPA-enhanced MRI. Similarly, our study results demonstrated that 11% of patients changed in the initial T stage and 4% of patients changed in Milan criteria after using CBCT-HA due to the detection of small, barely visible intrahepatic HCC on CT.

In our study, CBCT-HA during TACE with two-year imaging and clinical follow-up allowed the establishment of novel reference standard for hypervascular HCC, which included many sub-centimeter-sized HCCs which pre-existed initially, but clinically manifested as IDR on CT. This study helps to understand the nature of IDR and early stage HCC development. Our study showed that 120 of 148 (81.1%) and 148 of 256 (57.8%) of IDR during the one-year and two-year follow-up already existed on initial CBCT-HA, respectively. In theory, intrahepatic recurrence of HCC is attributable to two different mechanisms: metastasis in the early phase, and *de novo* primary HCC in the late phase. A previous study by Imamura et al. (27) reported that different variables associated with metastatic recurrence were responsible for early (< 2 years) phase recurrence; however, those related to elevated carcinogenesis contributed to late (≥ 2 years) phase recurrence, that also provided epidemiological evidence for the hypothesis. Our study results suggested that a large proportion of the HCCs, which were considered intrahepatic recurrences by metastasis in the early phase, may have been present initially without demonstration in conventional CT.

This study had several limitations. First, a selection bias was inevitable due to the retrospective design; our patient population had at least one possible HCC lesion
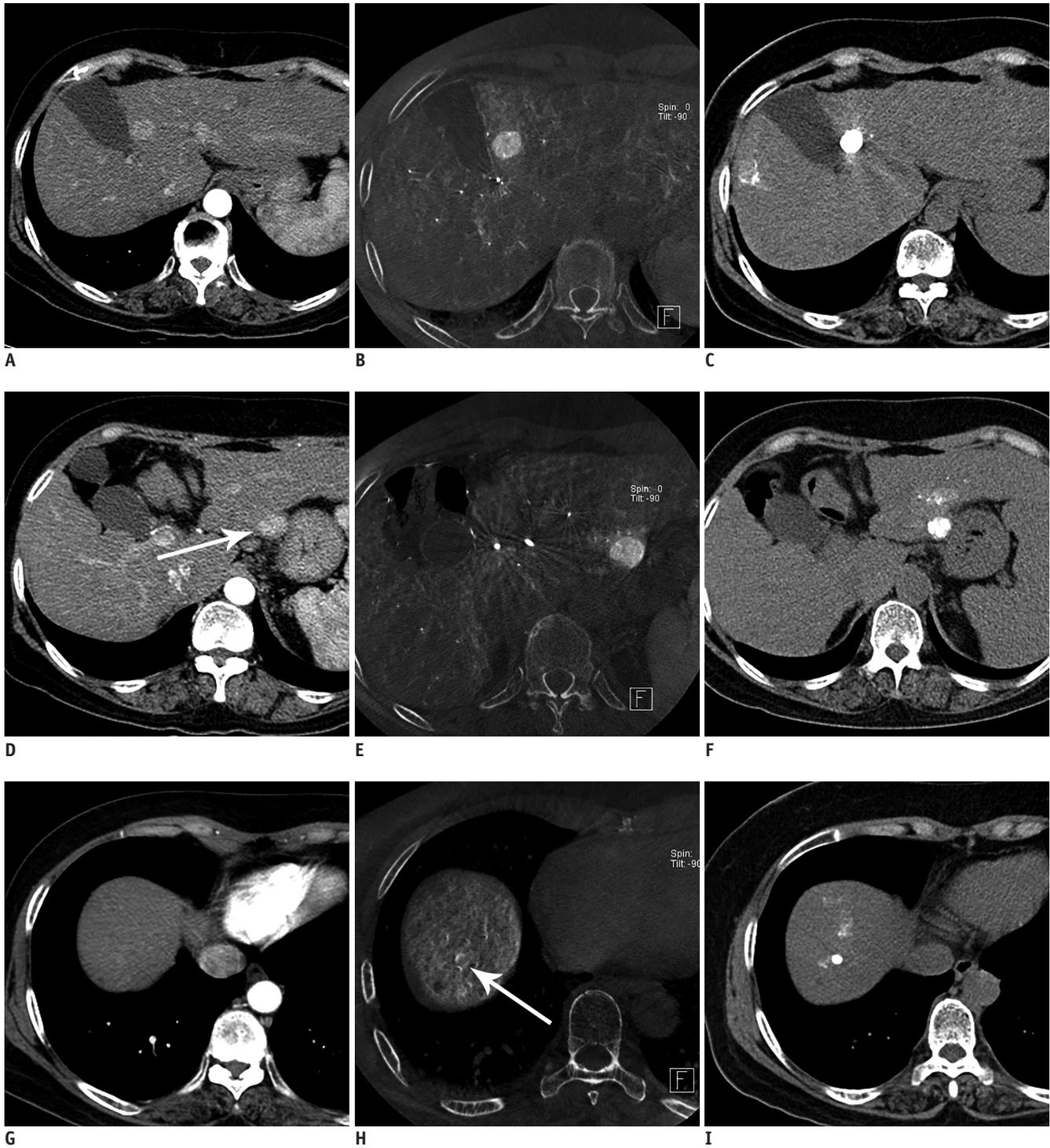
Fig. 3. 62-year-old woman with overt HCCs on initial dynamic CT and multiple hidden (additional hypervascular) foci seen on CBCT-HA.
(**A-F**; Group I) Two overt HCC lesions on initial dynamic CT (**A** and **D** [arrow] on arterial phase) revealed strongly enhancing nodules on initial CBCT-HA **(B, E)**. They were treated with TACE and demonstrated compact Lpiodol Ultra Fluide (Laboratoire Guerbet) uptake on immediate post-TACE non-contrast CT **(C, F)**. (**G-I**; Group II) Initial CBCT-HA revealed one additional enhancing nodule (arrow) **(H)** which was not depicted on initial dynamic CT **(G)**. Nodule was selectively treated with TACE and demonstrated compact Lipiodol uptake on immediate post-TACE non-contrast CT. CBCT-HA = cone-beam computed tomography-hepatic arteriography
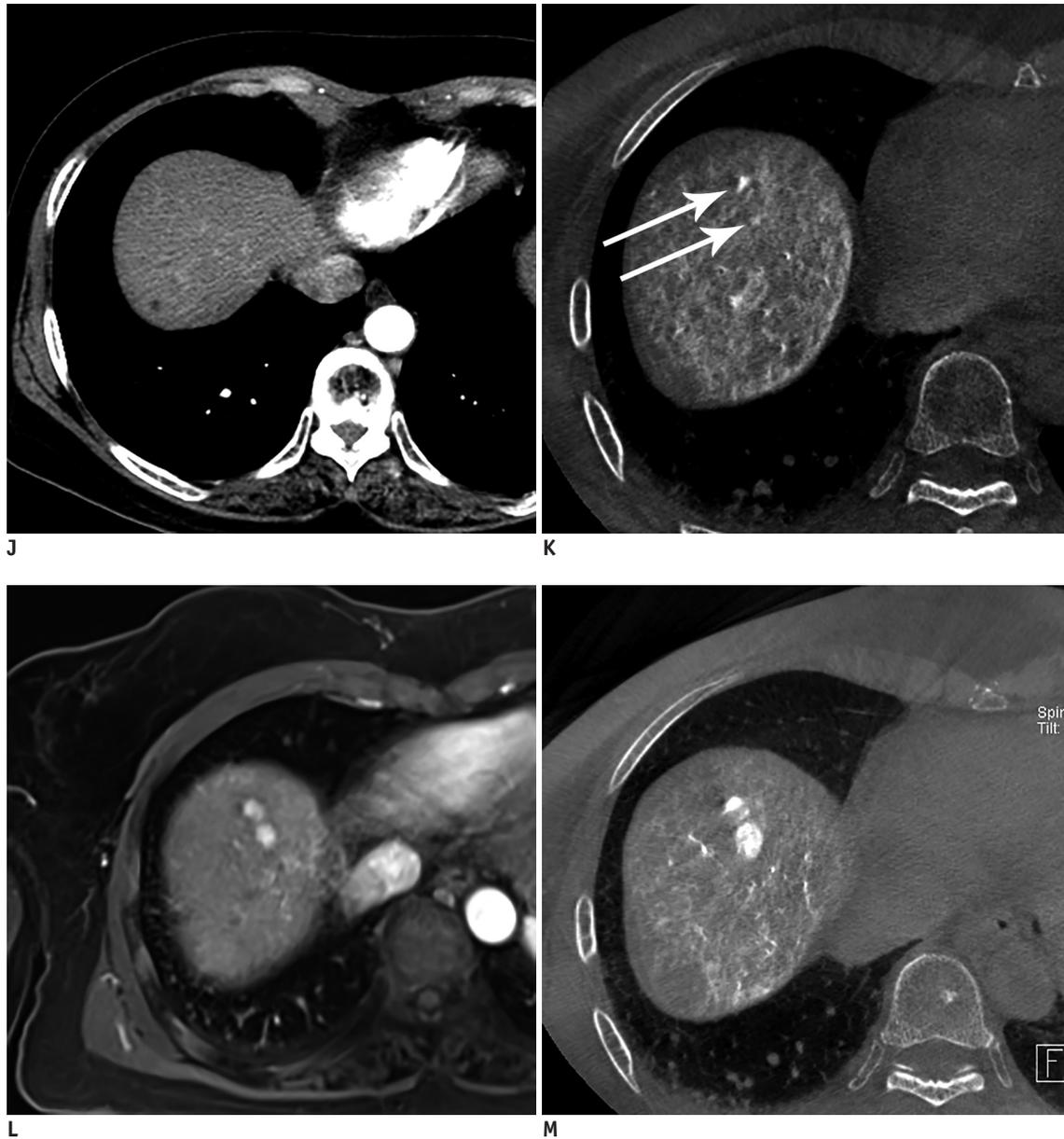
Fig. 3. 62-year-old woman with overt HCCs on initial dynamic CT and multiple hidden (additional hypervascular) foci seen on CBCT-HA.
(J-M; Group III) Twenty months later, two overt recurrent HCCs were found on dynamic liver MRI **(L)** and CBCT-HA **(M)**. On retrospective review of initial dynamic CT **(J)** and CBCT-HA **(K)**, two tiny enhancing foci (arrows) seen on initial CBCT-HA at sites match exactly with location of recurrent tumors. Follow-up CBCT-HA **(M)** demonstrated interval growth of those tiny enhancing foci. CBCT-HA = cone-beam computed tomography-hepatic arteriography

suspected at the prior surveillance examination. Second, a pathologic confirmation for the diagnosis of HCC was not used in our study. Instead, we established the novel reference standard for the diagnosis of HCC using CBCT-HA, and long-term follow up data with typical imaging features observed in dynamic CT or MRI after interval growth, and persistent iodized oil uptake after TACE, in addition to elevated AFP. No pathologic proof was provided; however, we assumed that methods established for the diagnosis of

HCC, including pre-existing hypervascular foci, would be the only practical methods used in a clinical setting. Third, extrahepatic collateral supplying HCC was not depicted on CBCT-HA because of the intra-arterial injection of contrast media into the common hepatic artery, and a limited field of view of CBCT; consequently, we excluded patients with multiple injections required for whole liver scanning. Furthermore, the motion artifact more severely affects the quality of CBCT-HA than MDCT images. These limitations

Table 3. Impact of CBCT-Based Novel Standard on Initial Tumor Staging and IDR

Initial Tumor Stage		Proportion of Preexisting HCCs in Initial CBCT-HA to IDR			
		One-Year Follow-Up, %		Two-Year Follow-Up, %	
Based on Dynamic CT	Based on CBCT-Based Novel Standard	Per Lesion	Per Person	Per Lesion	Per Person
Single HCC within Milan (n = 61)	Single HCC within Milan (n = 38)	50.0 (4/8)	57.1 (4/7)	12.9 (4/31)	28.6 (4/14)
	Multiple HCCs within Milan (n = 17)	83.3 (20/24)	100 (15/15)	47.8 (22/46)	100 (17/17)
	Multiple HCCs beyond Milan (n = 6)	92.3 (24/26)	100 (6/6)	79.1 (34/43)	100 (6/6)
Single HCC beyond Milan (n = 4)	Single HCC beyond Milan (n = 2)	0 (0/2)	0 (0/1)	0 (0/5)	0 (0/2)
	Multiple HCCs beyond Milan (n = 2)	66.7 (2/3)	100 (2/2)	25.0 (2/8)	100 (2/2)
Multiple HCCs within Milan (n = 24)	Multiple HCCs within Milan (n = 13)	40.0 (2/5)	50.0 (2/4)	45.5 (5/11)	62.5 (5/8)
	Multiple HCCs beyond Milan (n = 11)	91.5 (54/59)	100 (8/8)	80.7 (67/83)	100 (11/11)
Multiple HCCs beyond Milan (n = 10)	Multiple HCCs beyond Milan (n = 10)	66.7 (14/21)	85.7 (6/7)	48.3 (14/29)	75.0 (6/8)
Total (n = 99)	-	81.1 (120/148)	86.0 (43/50)	57.8 (148/256)	75.0 (51/68)

IDR = intrahepatic distant recurrence

could decrease the performance of CBCT-HA; however, they can be overcome in clinical practice by a careful search for extrahepatic collaterals together with adequate patient cooperation. Last, IDR can alternatively be defined as the development of new lesion after initial TACE from a clinical point of view, as described in the Results section. Therefore, further research is needed on this different interpretation of IDR.

In conclusion, CBCT-HA during chemoembolization with two-year imaging and clinical follow-up allowed the establishment of novel reference standard for hypervascular HCCs. The high spatial and contrast resolution of CBCT-HA enabled the confirmation of many sub-centimeter-sized, faintly vascularized HCC nodules that pre-existed initially, but clinically manifested as IDR. These factors help in understanding the nature of IDR and the early development of HCC, as well as the clinical implications of changes in tumor staging and treatment decision.

Conflicts of Interest

The authors have no potential conflicts of interest to disclose.

ORCID iDs

Jin Wook Chung
  https://orcid.org/0000-0002-1090-6872
Ye Ra Choi
  https://orcid.org/0000-0002-2455-1718
Jung Hoon Kim
  https://orcid.org/0000-0002-8090-7758
Hyo-Cheol Kim
  https://orcid.org/0000-0002-6016-247X
Hwan Jun Jae
  https://orcid.org/0000-0002-0328-3400
Saebeom Hur
  https://orcid.org/0000-0003-0787-5101

REFERENCES

1. El-Serag HB, Rudolph KL. Hepatocellular carcinoma: epidemiology and molecular carcinogenesis. *Gastroenterology* 2007;132:2557-2576
2. Shimizu A, Ito K, Koike S, Fujita T, Shimizu K, Matsunaga N. Cirrhosis or chronic hepatitis: evaluation of small (≤2-cm) early-enhancing hepatic lesions with serial contrast-enhanced dynamic MR imaging. *Radiology* 2003;226:550-555
3. Kim JE, Kim SH, Lee SJ, Rhim H. Hypervascular hepatocellular carcinoma 1 cm or smaller in patients with chronic liver disease: characterization with gadoxetic acid-enhanced MRI that includes diffusion-weighted imaging. *AJR Am J Roentgenol* 2011;196:W758-W765
4. Borzio M, Borzio F, Macchi R, Croce AM, Bruno S, Ferrari A, et al. The evaluation of fine-needle procedures for the diagnosis of focal liver lesions in cirrhosis. *J Hepatol* 1994;20:117-121

5. Stigliano R, Burroughs AK. Should we biopsy each liver mass suspicious for HCC before liver transplantation?–No, please don't. *J Hepatol* 2005;43:563-568

6. Tan CH, Low SCA, Thng CH. APASL and AASLD consensus guidelines on imaging diagnosis of hepatocellular carcinoma: a review. *Int J Hepatol* 2011;2011:519783

7. Bhartia B, Ward J, Guthrie JA, Robinson PJ. Hepatocellular carcinoma in cirrhotic livers: double-contrast thin-section MR imaging with pathologic correlation of explanted tissue. *AJR Am J Roentgenol* 2003;180:577-584

8. Forner A, Vilana R, Ayuso C, Bianchi L, Solé M, Ayuso JR, et al. Diagnosis of hepatic nodules 20 mm or smaller in cirrhosis: prospective validation of the noninvasive diagnostic criteria for hepatocellular carcinoma. *Hepatology* 2008;47:97-104

9. Addley HC, Griffin N, Shaw AS, Mannelli L, Parker RA, Aitken S, et al. Accuracy of hepatocellular carcinoma detection on multidetector CT in a transplant liver population with explant liver correlation. *Clin Radiol* 2011;66:349-356

10. Wald C, Russo MW, Heimbach JK, Hussain HK, Pomfret EA, Bruix J. New OPTN/UNOS policy for liver transplant allocation: standardization of liver imaging, diagnosis, classification, and reporting of hepatocellular carcinoma. *Radiology* 2013;266:376-382

11. Miyayama S, Matsui O, Yamashiro M, Ryu Y, Takata H, Takeda T, et al. Detection of hepatocellular carcinoma by CT during arterial portography using a cone-beam CT technology: comparison with conventional CTAP. *Abdom Imaging* 2009;34:502-506

12. Kakeda S, Korogi Y, Ohnari N, Moriya J, Oda N, Nishino K, et al. Usefulness of cone-beam volume CT with flat panel detectors in conjunction with catheter angiography for transcatheter arterial embolization. *J Vasc Interv Radiol* 2007;18:1508-1516

13. Miyayama S, Yamashiro M, Okuda M, Yoshie Y, Sugimori N, Igarashi S, et al. Usefulness of cone-beam computed tomography during ultraselective transcatheter arterial chemoembolization for small hepatocellular carcinomas that cannot be demonstrated on angiography. *Cardiovasc Intervent Radiol* 2009;32:255-264

14. Meyer BC, Frericks BB, Voges M, Borchert M, Martus P, Justiz J, et al. Visualization of hypervascular liver lesions during TACE: comparison of angiographic C-arm CT and MDCT. *AJR Am J Roentgenol* 2008;190:W263-W269

15. Sze DY, Razavi MK, So SK, Jeffrey RB Jr. Impact of multidetector CT hepatic arteriography on the planning of chemoembolization treatment of hepatocellular carcinoma. *AJR Am J Roentgenol* 2001;177:1339-1345

16. Akpek S, Brunner T, Benndorf G, Strother C. Three-dimensional imaging and cone beam volume CT in C-arm angiography with flat panel detector. *Diagn Interv Radiol* 2005;11:10-13

17. Lee IJ, Chung JW, Yin YH, Kim HC, Kim YI, Jae HJ, et al. Cone-beam CT hepatic arteriography in chemoembolization for hepatocellular carcinoma: angiographic image quality and its determining factors. *J Vasc Interv Radiol* 2014;25:1369-1379. e1

18. Lee IJ, Chung JW, Yin YH, Kim HC, Kim YI, Jae HJ, et al. Cone-beam computed tomography (CBCT) hepatic arteriography in chemoembolization for hepatocellular carcinoma: performance depicting tumors and tumor feeders. *Cardiovasc Intervent Radiol* 2015;38:1218-1230

19. Mazzaferro V, Regalia E, Doci R, Andreola S, Pulvirenti A, Bozzetti F, et al. Liver transplantation for the treatment of small hepatocellular carcinomas in patients with cirrhosis. *N Engl J Med* 1996;334:693-700

20. Brierley JD, Gospodarowicz MK, Wittekind C. *TNM classification of malignant tumours*, 8th ed. Oxford: John Wiley & Sons, Ltd, 2017

21. Higashihara H, Osuga K, Onishi H, Nakamoto A, Tsuboyama T, Maeda N, et al. Diagnostic accuracy of C-arm CT during selective transcatheter angiography for hepatocellular carcinoma: comparison with intravenous contrast-enhanced, biphasic, dynamic MDCT. *Eur Radiol* 2012;22:872-879

22. Iwazawa J, Ohue S, Hashimoto N, Abe H, Hamuro M, Mitani T. Detection of hepatocellular carcinoma: comparison of angiographic C-arm CT and MDCT. *AJR Am J Roentgenol* 2010;195:882-887

23. Jin YJ, Nah SY, Lee JW, Lee JI, Jeong S, Lee DH, et al. Utility of adding Primovist magnetic resonance imaging to analysis of hepatocellular carcinoma by liver dynamic computed tomography. *Clin Gastroenterol Hepatol* 2013;11:187-192

24. Yoo SH, Choi JY, Jang JW, Bae SH, Yoon SK, Kim DG, et al. Gd-EOB-DTPA-enhanced MRI is better than MDCT in decision making of curative treatment for hepatocellular carcinoma. *Ann Surg Oncol* 2013;20:2893-2900

25. Choi SH, Byun JH, Kwon HJ, Ha HI, Lee SJ, Kim SY, et al. The usefulness of gadoxetic acid-enhanced dynamic magnetic resonance imaging in hepatocellular carcinoma: toward improved staging. *Ann Surg Oncol* 2015;22:819-825

26. El-Serag HB, Marrero JA, Rudolph L, Reddy KR. Diagnosis and treatment of hepatocellular carcinoma. *Gastroenterology* 2008;134:1752-1763

27. Imamura H, Matsuyama Y, Tanaka E, Ohkubo T, Hasegawa K, Miyagawa S, et al. Risk factors contributing to early and late phase intrahepatic recurrence of hepatocellular carcinoma after hepatectomy. *J Hepatol* 2003;38:200-207